İSTANBUL UNIVERSITY PRESS

Coğrafya Dergisi
Journal of Geography

Coğrafya Dergisi–Journal of Geography
JGEOGRAPHY 2025, (50): 39–46

https://doi.org/10.26650/JGEOG2025-1568294

Submitted: 16.10.2024
Revision Requested: 02.01.2025
Last Revision Received: 15.03.2025
Accepted: 19.03.2025

Research Article

Open Access

Assessing the Interaction Between Agricultural, Hydrological, and Meteorological Droughts in the Tigris River Basin

Khalil Valizadeh Kamran [1], Ayat Khaleel Dhiab [1] & Hala Abdulkareem [1]

[1] University of Tabriz, Remote sensing and GIS Department, Tabriz, Iran

Abstract

Drought is a common meteorological phenomenon that can result in a range of adverse outcomes. The Tigris River Basin (TRB) is located in the arid and semi-arid regions of southwestern Asia, where drought conditions have been observed to intensify. This research aims to understand the relationship between agricultural, hydrological, and meteorological droughts in the basin. To examine meteorological, agricultural, and hydrological droughts, the study employed three indicators: the Standardised Precipitation Index (SPI), derived from Terraclimate precipitation data; the Tasselled Cap greenness index, calculated from Terra-Moderate Resolution Imaging Spectroradiometer (MODIS) multispectral imagery; and surface water area fluctuations based on the MODIS Terra Daily normalised difference water index (NDWI). Our analysis of monthly SPI data from 2003 to 2022 indicates that approximately half of the months experienced meteorological drought conditions. The occurrence of agricultural drought was found to be associated with both 6-month and 21-month accumulation periods of SPI values, underscoring the intricate interrelationship between precipitation deficits and other influential factors in the context of agricultural drought. Hydrological droughts demonstrated significant correlations with meteorological droughts over accumulation periods of 1, 3and 15 months, indicating a rapid onset but prolonged impact on water resources. Our findings indicate that although the various types of drought are interconnected, their relationships are not straightforward. Further research is required to explore the factors driving these patterns.

Keywords Drought · Remote sensing · Tigris River basin

Citation: Kamran, K. V., Dhiab, A. K. & Abdulkareem, H. (2025). Assessing the interaction between agricultural, hydrological, and meteorological droughts in the Tigris River basin. *Coğrafya Dergisi–Journal of Geography*, (50), 39-46. https://doi.org/10.26650/JGEOG2025-1568294

Corresponding author: Khalil Valizadeh Kamran valizadeh@tabrizu.ac.ir

Introduction

Drought, defined as a water deficit relative to normal hydroclimatic conditions, is a common meteorological phenomenon, and its duration is expressed in years, months, or weeks (Mishra & Singh, 2010). Droughts can lead to significant environmental challenges, including water and food crises(Mdemu, 2021), forest loss (Knutzen et al., 2023), and threats to socioeconomic security(Yang, Liao, Di, & Shi, 2023). According to the World Meteorological Organisation (WMO) and the United Nations Convention to Combat Desertification (UNCCD), weather-, climate-, and water-related hazards have accounted for 50% of all disasters and 45% of all deaths worldwide since 1970 (Douris & Kim, 2021). As climate change continues to persist and intensify, many regions worldwide are anticipated to encounter more frequent and severe droughts, with irreversible consequences for both human and natural ecosystems (Boloorani et al., 2024a). These developments underscore the critical importance of drought as an extreme event.

Drought is classified into four principal categories based on its impact: meteorological drought (relating to precipitation anomalies), agricultural drought (affecting soil moisture and crop yields), hydrological drought (impacting surface and groundwater resources), and socioeconomic drought (influencing human water needs and communities) (Svoboda, Hayes, & Wood, 2012). These categories are interrelated, and their definitions are linked to their specific impacts and measurement methods (Zeng et al., 2022). It is noteworthy that the majority of drought effects correspond to agricultural or hydrological droughts, as human communities and ecosystems rely more heavily on water reserves such as soil moisture, aquifers, lakes, and rivers than on direct precipitation (Van Loon & Laaha, 2015). Thus, a comprehensive understanding of drought types and their interrelations is crucial for developingeffective drought management and mitigation strategies.

From the beginning of the 21st century, there has been a notable global increase in both the frequency and duration of drought events, with a reported 29% increase worldwide (Douris & Kim, 2021). This trend is particularly evident in the Middle East and Southwest Asia, where the intensification of droughts has resulted in a cascade of environmental challenges. These include the desiccation of lakes and wetlands, the abandonment of agricultural lands because of reduced soil moisture and water availability, and the subsequent formation of dust emission sources(Boloorani et al., 2024a). The interconnected nature of these effects underscores the complex and multifaceted challenges of increasing drought frequency and persistence in vulnerable regions.

In recent years, the Tigris River basin (TRB) has experienced significant impacts from reduced rainfall and increased evaporation, leading to persistent water shortages in both river flows and groundwater reserves (Chang & Niu, 2023). The TRB's diverse geography and climate contribute to an imbalanced distribution of water resources across the region(Köle, 2017). This inherent disparity in water availability is further exacerbated by human activities, including the construction of dams and the implementation of water diversion schemes, which intensify the natural imbalance in water distribution throughout the basin (UNESCWA, 2013).

Despite the significant implications of drought in the TRB for the environment, agriculture, and human populations, this critical issue has not received sufficient attention. The lack of focus on drought in this region is particularly troubling considering its far-reaching and multifaceted impacts across various sectors. Understanding the process by which meteorological drought evolves into other forms of drought-a process referred to as drought propagation-is essential for mitigating the negative impacts of ensuing drought conditions (Xu, Wu, Shao, He, & Guo, 2023). This knowledge enables the formulation of more effective preparedness and response strategies to address the various consequences of prolonged dry periods (Boloorani et al., 2024a). To achieve this, this study employs multi-temporal and multi-sensor remote sensing data to assess the interaction between agricultural, hydrological, and meteorological droughts in the TRB.

Study Area

The Tigris River, a major waterway in the Middle East, traverses a basin shared by four countries. The distribution of the river course is as follows: Türkiye(24.5%), Syria (0.4%), Iraq (56.1%), and Iran (19%). The basin covers an area of approximately 221,000 square kilometres and is situated within the following coordinates: 30° 59' to 38° 44' North latitude and 39° 8' to 48° 24' East longitude. The region is confronted with significant challenges pertaining to water resources, including concerns regarding quantity, quality, and biodiversity (Bachmann, Tice, Al-Obeidi, & Kılıç, 2019). Furthermore, climate change projections for the TRB indicate a troubling trend, with anticipated reductions in precipitation and river flow, coupled with rising temperatures (Al-Taei, Alesheikh, & Darvishi Boloorani, 2023). Figure 1 shows the location map of the TRB.

Figure 1

Location map of the TRB

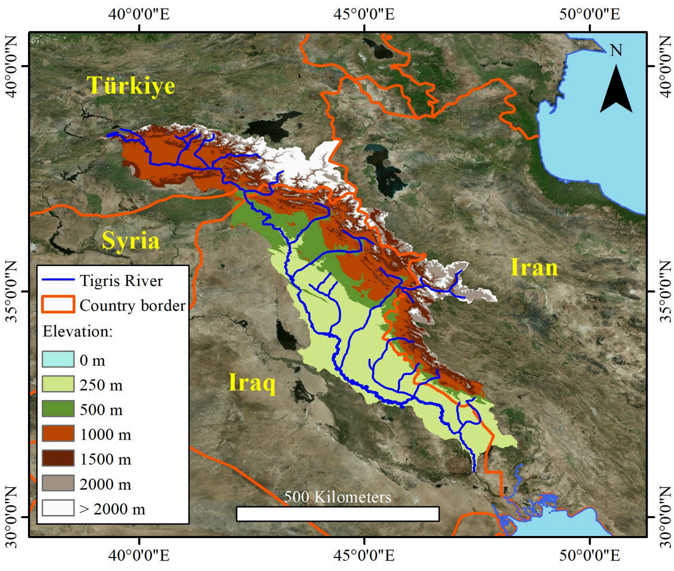

Reproduced from Haghighi et al. (2023) under an open-access license.

Source: Haghighi et al. 2023

Materials and Methods

Satellite-based drought monitoring

Satellite-based drought monitoring is a valuable and effective tool for assessing and monitoring drought conditions over extensive areas with high spatial and temporal resolution. This approach employs remote sensing indices and data products to quantify vegetation, soil moisture, and water storage (Behifar, Kakroodi, Kiavarz, & Azizi, 2023). Satellite-based drought monitoring techniques offer several benefits, including consistent coverage of remote or inaccessible regions and the ability to provide near-real-time data (Alahacoon, Edirisinghe, & Ranagalage, 2021). Consequently, satellite-based drought monitoring represents a fundamental component of drought warning systems and agricultural management strategies.

Assessing meteorological droughts

A prolonged shortage of rainfall is typically defined as a meteorological drought. In this study, we use the standardized precipitation index (SPI) (McKee, Doesken, & Kleist, 1993) to quantify and monitor the spatial and temporal patterns of meteorological drought. In our analysis, we used the Terr climate precipitation dataset (Abatzoglou, Dobrowski, Parks, & Hegewisch, 2018) to collate rainfall data from 2001/01 to 2022/12. Subsequently, precipitation accumulation was calculated for accumulation periods of 1, 3, 6, 9, 12, 15, 18, 21, and 24 months. Given that precipitation is typically distributed according to a gamma distribution (Martinez-Villalobos & Neelin, 2019), the data were normalised by fitting it to a gamma probability distribution function, as introduced by Laimighofer and Laaha (2022). Finally, the SPI was calculated for each accumulation period by subtracting the mean value from each pixel and dividing by the standard deviation. (Laimighofer & Laaha, 2022)

Analysing agricultural droughts

Agricultural drought is defined as a condition in which the soil moisture content falls below the critical level required for crop sustenance. This condition can be identified by examining soil moisture characteristics and the physicochemical attributes of crops throughout the growing period (Liu et al., 2016). A soil moisture deficiency canreduce the available water supply, which may be insufficient to meet the essential physiological needs of crops. This can lead to a suppression of crop growth, which in turn can result in reduced yields or even complete crop failure(Bhattacharya & Bhattacharya, 2021).

To evaluate the impact of drought on agricultural production in the TRB region, we employed the "greenness" component derived from the Tasselled Cap transformation, which is based on the Terra-Moderate Resolution Imaging Spectroradiometer (MODIS) multispectral data. This transformation involves applying linear combinations of spectral bands, where each band is multiplied by its specific constant coefficient. For the purposes of our analysis, we utilised the coefficients established by Zhang et al. (2002) for the MODIS bands (Table 1).

Table 1

Modis Nadir Bidirectional Reflectance Distribution Function-Adjusted Reflectance (NBAR) Tasselled Cap coefficients (Zhang et al., 2002)

Band	Wavelength (nm)	Coefficient
Nadir_Reflectance_Band1	620-670	-0.3399
Nadir_Reflectance_Band2	841-876	0.5952
Nadir_Reflectance_Band3	459-479	-0.2129
Nadir_Reflectance_Band4	545-565	-0.2222
Nadir_Reflectance_Band5	1230-1250	0.4617
Nadir_Reflectance_Band6	1628-1652	-0.1037
Nadir_Reflectance_Band7	2105-2155	-0.4600

To define the agricultural land boundary, the most frequent value of the LC_Type1 band of the MCD12Q1.061 dataset (Friedl & Sulla-Menashe, 2022) was calculated for each pixel. Subsequently, all pixels identified as croplands within the dataset were selected, provided that at least 24% of the area was classified as cultivated cropland (Figure 2). Once the agricultural land boundary had been defined for the region, the time series of agricultural land greenness between the years 2003 and 2022 (the maximum range of available data) was calculated using the coefficients from Table 1 and the monthly average of the MCD43A4.061 dataset (Schaaf & Wang, 2021).

Figure 2

Defined agricultural land boundary in the study area

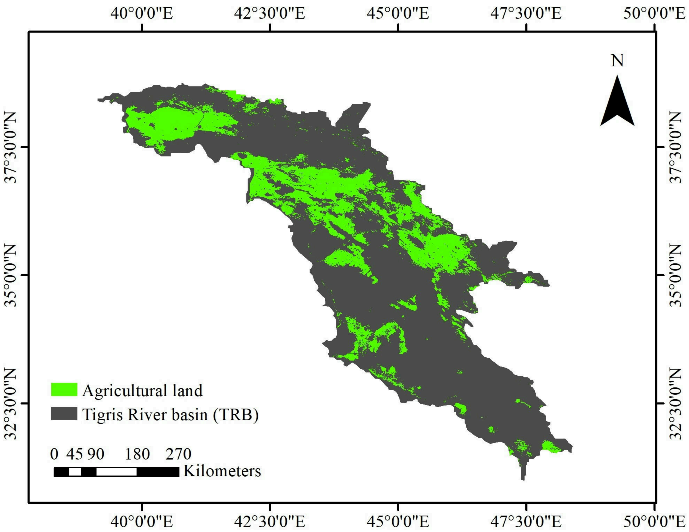

Hydrological drought analysis

A deficiency of water in the hydrological cycle results in hydrological drought, which is primarily caused by climate variability, specifically anomalies in precipitation and temperature. This water shortage is typically evidenced by a number of indicators, including unusually low river flows, reduced water levels in lakes and reservoirs, and depleted groundwater resources (Boloorani et al., 2024a, Kale, 2021a).

Despite the absence of consensus on the optimal method for measuring hydrological drought, there is a clear and direct correlation between precipitation and surface water flow, as evidenced by(McFeeters, 1996, Kale, 2021b).Considering this relationship, it is feasible to use alterations in the surface water area across the entire basin as a proxy for the assessment and quantification of hydrological drought conditions. To extract monthly surface water areas between 2003/01 and 2022/12, the MODIS Terra Daily normalised difference water index (NDWI) dataset with a pixel size of 463.313 metres was used. In accordance with the existing literature(Ji, Zhang, & Wylie, 2009), each pixel with an NDWI value greater than 0.1 was considered a surface water area.

Analysing drought propagation

Agricultural and hydrological droughts typically follow meteorological droughts, which are defined by abnormal precipitation and temperature patterns with specific time lags (Boloorani et al., 2024a). To identify the precise point of occurrence of all types of droughts subsequent to the onset of the meteorological drought and analyse their sequential occurrence, the cross-correlation method can be employed (Xu et al., 2023). This approach involves the calculation of the Pearson correlation coefficient between greenness (agricultural drought) and surface water areas (hydrological drought) in conjunction with SPI values (for accumulation periods of 1, 3, 6, 9, 12, 15, 18, 21, and 24 months). To ascertain greenness, the value of each month is added to the value of the previous month, resulting in a value ranging from 1 to 24. Figure 3 depicts the methodology employed in this study for drought propagation.

Results and Discussion

The most severe meteorological droughts, as indicated by the lowest SPI values, occurred in August, July, September, and

Figure 3

Utilised research framework in the study

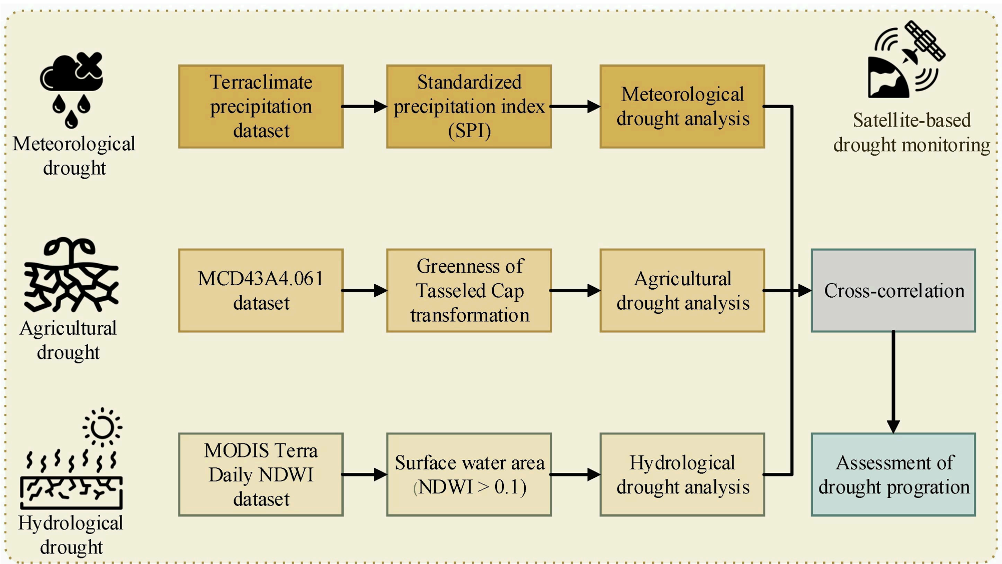

June. In contrast, the months with the highest precipitation levels, which corresponded to the highest SPI values, were January, March, and February, respectively. Furthermore, the lowest levels of greenness were observed in January, December, and November, whereas April, May, and June exhibited the highest levels of greenness. Finally, the lowest surface water area was observed in July, August, and September, whereas the highest surface water area was observed in February, January, and March. Therefore, an analysis of the monthly drought indicators revealed no significant temporal consistency in the drought types under study. Figure 4 illustrates the monthly values of the measured satellite-based drought indices.

In accordance with the established patterns of monthly droughts, an analysis of the average annual drought indicators demonstrated a notable absence of substantial temporal consistency among the various types of droughts under investigation. On an annual scale, similar to (Boloorani et al., 2024b), the most pronounced drought conditions (based on the SPI) occurred in the years 2021 (-0.327), 2022 (-0.187), and 2008 (-0.164). In contrast, the highest precipitation levels were observed in 2018 (0.214), 2016 (0.130), and 2006 (0.113). Tasselled Cap greenness, which serves as a proxy for agricultural activities, reached its highest point in 2019 (749.8 × 10^4), followed by 2020 (624.8 × 10^4) and 2016 (523.0 × 10^4). In contrast, the lowest greenness values were recorded in 2008 (285.5 × 10^4), 2012 (344.6 × 10^4), and 2005 (364.4 × 10^4). The maximum extent of surface water was observed in 2019 (2.98 × 10^{-3} km²), followed by 2007 (2.87 × 10^{-3} km²) and 2003 (2.81 × 10^{-3} km²). The lowest surface water extents were observed in 2010 (1.78 × 10^{-3} km²), 2021 (1.84 × 10^{-3} km²), and 2022 (2.24 × 10^{-3} km²).

Meteorological drought

The SPI is an efficient tool for gauging meteorological drought. A positive SPI value indicates that precipitation exceeded the median, whereas a negative SPI value signifies that precipitation fell below the median, indicating dry conditions (Khan, Gabriel, & Rana, 2008). In accordance with the SPI thresholds delineated in Table 2 and the mean cumulative SPI values at a 1-month interval from 2003 to 2022, the TRB is subject to moderate drought conditions from June to September. The month of October has mild drought conditions, while the remaining months exhibit mild wet

Figure 4

Monthly drought index values

SPI: Highest value / Lowest value

	2003	2004	2005	2006	2007	2008	2009	2010	2011	2012	2013	2014	2015	2016	2017	2018	2019	2020	2021	2022
Jan	0.84	1.17	1.07	1.22	0.59	0.67	0.34	0.92	0.94	0.80	1.26	0.97	0.42	1.20	0.69	0.89	1.20	1.05	0.76	1.04
Feb	1.23	0.99	0.93	1.29	0.79	0.79	0.88	0.99	0.73	1.04	0.71	0.30	0.76	0.89	0.51	1.09	0.97	1.17	0.62	0.49
Mar	1.20	0.58	0.98	0.68	0.93	0.13	0.97	0.78	0.84	0.75	0.84	1.06	0.92	1.09	1.03	0.66	1.30	1.25	0.64	0.63
Apr	0.99	0.91	0.67	1.09	1.20	-0.05	0.85	0.94	1.21	0.72	0.71	0.47	0.35	0.98	1.03	0.96	1.11	0.81	-0.38	0.17
May	-0.32	0.71	0.22	-0.04	0.07	-0.25	-0.49	0.57	0.54	0.11	0.63	0.01	0.16	0.42	0.40	0.94	0.25	0.30	-0.45	0.01
Jun	-0.95	-1.20	-1.05	-1.32	-1.06	-1.21	-0.91	-0.97	-1.08	-1.10	-1.17	-1.06	-0.87	-0.89	-1.27	-0.98	-1.19	-1.16	-1.33	-1.20
Jul	-1.27	-1.18	-1.29	-1.27	-1.18	-1.21	-1.18	-1.29	-1.14	-1.08	-1.31	-1.24	-1.31	-1.17	-1.31	-1.31	-1.32	-1.16	-1.31	-1.30
Aug	-1.25	-1.32	-1.25	-1.32	-1.20	-1.25	-1.26	-1.29	-1.28	-1.32	-1.30	-1.32	-1.18	-1.32	-1.28	-1.26	-1.25	-1.24	-1.24	-1.27
Sep	-1.24	-1.32	-1.23	-1.28	-1.34	-0.97	-0.92	-1.26	-1.01	-1.19	-1.22	-1.16	-1.23	-1.03	-1.30	-1.22	-1.28	-1.31	-1.30	-1.26
Oct	0.00	-0.62	-0.56	0.76	-0.66	0.53	0.19	-0.43	0.25	0.28	-0.84	0.55	0.74	-0.18	-0.45	0.55	-0.01	-1.11	-0.56	-0.55
Nov	1.03	1.21	0.72	0.85	0.25	0.49	1.16	-0.55	0.68	1.00	0.92	0.93	0.32	0.32	0.80	0.98	0.03	0.82	-0.10	0.86
Dec	1.03	0.50	0.82	0.70	0.74	0.36	0.91	0.46	0.25	1.17	0.93	0.67	0.94	1.23	0.40	1.28	1.05	0.41	0.74	0.15

Greenness × 10^4: Highest value / Lowest value

	2003	2004	2005	2006	2007	2008	2009	2010	2011	2012	2013	2014	2015	2016	2017	2018	2019	2020	2021	2022
Jan	184	366	186	164	104	154	177	379	233	206	311	352	424	438	223	257	707	437	344	205
Feb	297	417	195	207	233	117	308	493	222	153	543	473	541	510	163	344	898	492	466	192
Mar	451	660	457	366	456	208	436	693	352	140	734	749	686	791	366	621	1040	810	646	387
Apr	670	702	615	706	682	401	624	773	532	487	826	819	795	856	701	793	1133	1049	739	516
May	672	706	629	760	715	437	675	655	684	596	708	738	741	792	713	793	987	920	680	592
Jun	565	609	512	597	578	363	530	518	584	501	560	586	587	615	601	602	838	763	558	485
Jul	477	507	414	492	481	291	421	439	479	410	480	484	494	523	500	477	725	651	473	393
Aug	406	442	345	421	420	460	377	391	413	335	427	425	429	452	432	421	662	590	416	346
Sep	358	391	313	378	369	213	349	357	379	300	386	382	362	408	386	387	603	518	372	328
Oct	310	343	275	361	334	235	299	330	339	284	335	376	339	352	338	374	549	461	339	303
Nov	276	314	237	322	281	277	280	292	278	341	349	385	401	292	286	461	442	429	303	306
Dec	329	199	195	276	215	272	295	246	206	384	264	434	352	248	231	680	414	379	270	333

Surface water area × 10^-3 Km^2: Highest value / Lowest value

	2003	2004	2005	2006	2007	2008	2009	2010	2011	2012	2013	2014	2015	2016	2017	2018	2019	2020	2021	2022
Jan	5.79	5.99	7.03	7.05	8.81	7.17	5.72	4.06	5.80	5.32	7.37	5.78	5.95	6.71	5.47	4.38	6.51	5.68	4.87	6.71
Feb	7.65	7.36	8.26	7.29	7.11	7.23	5.08	5.06	6.25	7.49	5.59	5.26	5.34	5.53	7.64	5.68	6.09	6.46	5.19	5.62
Mar	6.09	3.73	5.19	4.46	4.69	4.35	5.33	3.44	4.75	7.09	4.51	5.07	4.84	5.27	6.28	2.92	7.64	5.50	3.97	4.86
Apr	4.45	3.12	3.46	3.70	4.69	1.43	3.78	2.61	3.77	3.44	2.89	2.87	3.14	3.56	3.93	2.78	5.88	3.55	2.14	2.89
May	1.67	1.81	1.69	1.60	1.99	0.86	1.69	1.49	1.61	1.28	2.12	1.35	1.76	1.64	1.69	2.06	2.58	2.05	0.63	1.49
Jun	0.38	0.38	0.41	0.25	0.33	0.17	0.56	0.31	0.41	0.23	0.41	0.33	0.43	0.42	0.31	0.44	0.70	0.47	0.17	0.34
Jul	0.15	0.28	0.11	0.16	0.18	0.12	0.10	0.10	0.19	0.15	0.15	0.16	0.13	0.15	0.15	0.16	0.38	0.34	0.17	0.11
Aug	0.14	0.15	0.16	0.24	0.19	0.28	0.10	0.14	0.12	0.10	0.14	0.17	0.19	0.15	0.15	0.13	0.40	0.22	0.25	0.17
Sep	0.15	0.13	0.22	0.15	0.10	0.75	0.50	0.19	0.33	0.14	0.14	0.22	0.29	0.12	0.17	0.18	0.27	0.20	0.12	0.28
Oct	0.80	0.64	0.77	2.04	0.69	1.26	0.84	0.61	1.09	1.17	0.39	1.80	1.67	0.48	0.47	1.65	0.82	0.26	0.49	0.87
Nov	2.56	3.66	1.56	2.35	1.68	1.29	2.84	0.26	3.24	2.00	2.11	2.74	2.03	1.01	1.89	2.63	0.81	1.64	0.81	1.94
Dec	3.89	5.79	3.10	3.94	3.98	2.99	3.43	3.05	3.55	4.61	7.32	3.91	5.37	5.50	3.42	4.99	3.64	2.77	3.32	1.65

conditions. Furthermore, drought conditions (SPI < 0) were identified in 110 (45.8%) of the 240 months analysed. The prevailing dry condition in the basin may result in various environmental challenges, including the generation of dust storm sources(Al-Taei, Alesheikh, & Darvishi Boloorani, 2024).

Table 2

Meteorological drought categorisation by SPI (Lloyd-Hughes & Saunders, 2002)

SPI value	The drought category
≥ 2.00	Extremely wet
1.50–1.99	Severely wet
1.00 to 1.49	Moderately wet
0–0.99	Mildly wet
0 to −0.99	Mild drought
1.00 to 1.49	Moderate drought
1.50 to 1.99	Severe drought
≤ -2.00	Extreme drought

meteorological droughts affect various water resources in different ways (McKee et al., 1993). For instance, soil moisture conditions respond rapidly to changes in precipitation, whereas groundwater levels, streamlet, and reservoir storage were influenced by longer-term precipitation patterns. Consequently, in the continuation of this work, we assessed the cumulative SPI at multiple time scales and measured its relationship with agricultural and hydrological droughts.

Agricultural drought

Agricultural droughts typically follow meteorological droughts, with the time delay varying based on local climate conditions and ecosystem factors (C.V, Pachore, & Remesan, 2024). Our observations indicate that meteorological and agricultural droughts coincided in 2008, and heavy rainfall in 2019 led to decreased and increased greenery, respectively. However, this pattern did not consistently occur over time.

The results of the cross-correlation analysis are presented in Table 3. Accordingly, the strongest correlation coefficients are observed between the 9-month (0.73), 6-month (0.66), 18-month (0.62), and 21-month (0.60) cumulative SPI and Tasselled Cap greenness. This observation indicates that agricultural drought is not a sole consequence of inadequate precipitation. In other words, the management of water resources and the implementation of agricultural strategies also play a pivotal role in determining the onset and severity of agricultural drought (Boloorani et al., 2024b; Smith & Edwards, 2021). Factors such as irrigation efficiency, crop selection, soil management, and the utilisation of water conservation techniques also influence how agricultural systems respond to dry periods (C.V et al., 2024). our methodology for delineating agricultural boundaries relied on MODIS annual land cover maps. This approach may have introduced certain limitations or biases into our results.

Hydrological drought

The surface water area was considered an indicator of hydrological drought. In accordance with the findings of the Tigris-Euphrates Rivers basin(Al-Taei et al., 2023)and precipitation data for Iraq(Al-Muhyi & Aleedani, 2022; Naqi, Al-Jiboori, & Al-Madhhachi, 2021; Rahi, Al-Madhhachi, & Al-Hussaini, 2019), multiple instances of hydrological drought were observed during the period 2003-2022. These instances were characterized by an increasing intensity of drought. The confluence of natural forces, including climate fluctuations, and human-induced factors, such as dam construction, irrigation practices, and inadequate water management strategies, contributes to the alteration of the water bodies of the TRB (Darvishi Boloorani et al., 2021).

To ascertain the relationship between meteorological and hydrological droughts, Pearson correlation coefficients between cumulative SPI values and surface water area were calculated (Table 4). Table 4 demonstrates the existence of robust, direct correlation between hydrological drought and both 1-month (0.83) and 3-month (0.79) cumulative SPI values. Although surface water area is a limited indicator of the severity of hydrological drought, given that the impact of precipitation variations on reservoir levels is minimal (Boloorani et al., 2024a), the aforementioned high correlations indicate a rapid translation of meteorological drought conditions into hydrological impacts. However, a moderate strength direct correlation (0.55) was observed between hydrological drought and 15-month cumulative SPI. This observation demonstrates that the effects of meteorological drought on water resources can persist for extended periods. It is crucial to note that there was a discrepancy in the spatial

Table 3

Pearson's correlation coefficient between cumulative SPI and total assessed cap greenness

	1-month	3-month	6-month	9-month	12-month	15-month	18-month	21-month	24-month
Pearson correlation coefficient	−0.01	0.28	0.66	0.73	0.32	0.36	0.62	0.60	0.30

Table 4

Pearson's correlation coefficient between cumulative SPI and surface water area

	1-month	3-month	6-month	9-month	12-month	15-month	18-month	21-month	24-month
Pearson correlation coefficient	0.83	0.79	0.36	−0.19	0.10	0.55	0.29	−0.11	0.09

resolution between the SPI maps and the delineated water area maps, which could influence the results.

Conclusion

This research examined how agricultural, hydrological, and meteorological droughts interact in the TRB region. To understand this, the study used long-term satellite data and statistical methods. The key findings of this work are as follows:

- During 2003 and 2022, nearly half of the SPI observations were meteorological drought-induced, confirming the general dry conditions in the basin.
- The occurrence of agricultural drought is strongly influenced by meteorological drought conditions over both the 6-month and 21-month accumulation periods, as indicated by the SPI. This demonstrates that agricultural drought in TRB is not solely a result of insufficient precipitation.
- The occurrence of hydrological drought shows a strong to moderate correlation with meteorological drought conditions over accumulation periods of 1, 3, and 15 months. This indicates that meteorological drought conditions can quickly affect water resources, and their effects can persist for extended periods.
- The drought progression analysis indicated that the drought types were not entirely correlated. Hence, further investigations are required to understand the factors influencing these patterns.

Ethics Committee Approval: Ethics committee approval is not required for the study.
Peer Review: Externally peer-reviewed.
Author Contributions: Conception/Design of Study- K.V.K., A.K.D., H.A.; Data Acquisition- K.V.K., A.K.D., H.A.; Data Analysis/Interpretation- K.V.K., A.K.D., H.A.; Drafting Manuscript- K.V.K., A.K.D., H.A.; Critical Revision of Manuscript- K.V.K., A.K.D., H.A.; Final Approval and Accountability- K.V.K., A.K.D., H.A.
Conflict of Interest: Authors declared no conflict of interest.
Grant Support: Authors declared no financial support.

Author Details

Khalil Valizadeh Kamran
[1] University of Tabriz, Remote sensing and GIS Department, Tabriz, Iran
0000-0003-4648-842X valizadeh@tabrizu.ac.ir

Ayat Khaleel Dhiab
[1] University of Tabriz, Remote sensing and GIS Department, Tabriz, Iran
0000-0001-5561-8025

Hala Abdulkareem
[1] University of Tabriz, Remote sensing and GIS Department, Tabriz, Iran
0009-0009-6100-0155

REFERENCES

Abatzoglou, J. T., Dobrowski, S. Z., Parks, S. A., & Hegewisch, K. C. (2018). TerraClimate, a high-resolution global dataset of monthly climate and climatic water balance from 1958–2015. *Scientific data, 5*(1), 1-12.

Al-Muhyi, A. H. A., and Aleedani, F. Y. K. (2022). Impacts of global climate change on temperature and precipitation in basra city, Iraq. *Basrah Journal of Sciences, 40*(1), 215-230.

Al-Taei, A. I., Alesheikh, A. A., &Boloorani, A. (2023). Land Use/Land Cover Change Analysis Using Multi-Temporal Remote Sensing Data: A Case Study of the Tigris and Euphrates Rivers Basin. *Land, 12*(5), 1101.

Al-Taei, A. I., Alesheikh, A. A., &Boloorani, A. (2024). Hazardous Dust Source Susceptibility Mapping in Wet and Dry Periods of the Tigris-Euphrates Basin: A Meta-Heuristics and Machine Learning. *Environmental Management Hazards, 10*(4), 355-370.

Alahacoon, N., Edirisinghe, M., & Ranagalage, M. (2021). Satellite-based meteorological and agricultural drought monitoring for agricultural sustainability in Sri Lanka. *Sustainability, 13*(6), 3427.

Bachmann, A., Tice, V., Al-Obeidi, L. A., & Kılıç, D. T. (2019). Tigris-Euphrates River ecosystem: A status report. In *Mesopotamia Water Forum*.

Behifar, M., Kakroodi, A. A., Kiavarz, M., & Azizi, G. (2023). Satellite-based drought monitoring using optimal indices for diverse climates and land types. *Ecological Informatics, 76*, 102143.

Bhattacharya, A., & Bhattacharya, A. (2021). Effects of soil water deficit on growth and development of plants: a review. *Soil water deficit and physiological issues in plants*, 393-488.

Boloorani, A. D., Soleimani, M., Papi, R., Nasiri, N., Samany, N. N., Mirzaei, S., & Al-Hemoud, A. (2024a). Assessing the role of drought in dust storm formation in the Tigris and Euphrates basin. *Science of The Total Environment, 921*, 171193.

Boloorani, A. D., Soleimani, M., Papi, R., Nasiri, N., Samany, N. N., Mirzaei, S., and Al-Hemoud, A. (2024b). Assessing the role of drought in dust storm formation in the Tigris and Euphrates basin. *Science of The Total Environment, 921*, 171193.

Chang, L.-L. and Niu, G.-Y. (2023). Impact of Interannual Climate Variability on the Declining Terrestrial Water Storage Trend over the Tigris–Euphrates River Basin. *Journal of Hydrometeorology, 24*(3), 549-560.

C.V, A., Pachore, A., & Remesan, R. (2024). Agricultural drought response to meteorological drought over different agro-climatic zones of the Ganga River basin. *Journal of Water and Climate Change, 15*(3), 998-1017.

Darvishi Boloorani, A., R. Papi, M. Soleimani, L. Karami, F. Amiri, and N. N. Samany (2021). Water body changes in the Tigris and Euphrates basins have affected the phenomenon of dust storms.*Aeolian Research, 50*, 100698.

Douris, J., & Kim, G. (2021). *The Atlas of Mortality and Economic Losses from Weather, Climate and Water Extremes (1970-2019)*. WMO, Switzerland. Retrieved from https://coilink.org/20.500.12592/b3d1n6

Friedl, M., & Sulla-Menashe, D. (2022). MODIS/Terra+ Aqua land cover type yearly L3 global 500 m SIN grid V061 [Data set]. *NASA EOSDIS Land Processes Distributed Active Archive Centre*. Retrieved from https://doi.org/10.5067/MODIS/MCD12Q1.061

Haghighi, A. T., Akbari, M., Noori, R., Mehr, A. D., Gohari, A., Sönmez, M. E., ... & Kløve, B. (2023). The impact of Turkey's water resource development on the flow regime of the Tigris River in Iraq. *Journal of Hydrology: Regional Studies*, *48*, 101454.

Ji, L., Zhang, L., & Wylie, B. (2009). Analysis of dynamic thresholds for the normalised difference water index. *Photogrammetric engineering & remote sensing, 75*(11), 1307-1317.

Kale, M. M. (2021a). Akarçay Kapalı Havzası için hidrolojik kuraklık analizi. *Coğrafya Dergisi*, (42), 165-180.

Kale, M. M. (2021b). Manavgat Çayı kuraklık analizi. *Ege Coğrafya Dergisi*, *30*(1), 107-123.

Khan, S., Gabriel, H., & Rana, T. (2008). Standard precipitation index to track drought and assess the impact of rainfall on water tables in irrigation areas. *Irrigation and Drainage Systems, 22*, 159-177.

Knutzen, F., Averbeck, P., Barrasso, C., Bouwer, L. M., Gardiner, B., Grünzweig, J. M., . . . Kollet, S. (2023). Impacts and damages of the European multi-year drought and heat event 2018–2022 on forests, a review. *Egusphere, 2023*, 1-56.

Köle, M. M. (2017). 1954–2016 DÖNEMİ TÜRKİYE SINIRAŞAN SULAR POLİTİKASI. *Marmara Coğrafya Dergisi*, (35), 122-133.

Laimighofer, J., & Laaha, G. (2022). How standard are standardised drought indices? Uncertainty components in the SPI & SPEI case. *Journal of Hydrology 613, 128385–128385*.

Liu, X., Zhu, X., Pan, Y., Li, S., Liu, Y., and Ma, Y. (2016). Agricultural drought monitoring: Progress, challenges, and prospects. *Journal of Geographical Sciences, 26*, 750-767.

Lloyd-Hughes, B., & Saunders, M. A. (2002). A drought climatology for Europe. *International Journal of Climatology, 22*(13), 1571-1592.

Martinez-Villalobos, C., and J. D. (2019). Why do precipitation intensities tend to follow gamma distributions? *J Atmos Sci. 76*(11), 3611-3631.

McFeeters, S. K. (1996). Use of the Normalised Difference Water Index (NDWI) for delineating open water features. *International journal of remote sensing, 17*(7), 1425-1432.

McKee, T. B., Doesken, N. J., & Kleist, J. (1993). The relationship of drought frequency and duration to time scales. In *Proceedings of the 8th Conference on Applied Climatology* (Vol. 17, No. 22, pp. 179-183).

Mdemu, M. V. (2021). 'Community's vulnerability to drought-driven water scarcity and food insecurity in central and northern semi-arid areas of Tanzania. *Frontiers in Climate, 3*, 737655.

Mishra, A. K., & Singh, V. P. (2010). A review of drought concepts. *J Hydrol.*, *391*(1-2), 202-216.

Naqi, N. M., Al-Jiboori, M. H., & Al-Madhhachi, A. S. T. (2021). Statistical analysis of extreme weather events in the Diyala River basin, Iraq. *Journal of Water and Climate Change, 12*(8), 3770-3785.

Rahi, K. A.; Al-Madhhachi, A.-S. T.; Al-Hussaini, S. N. (2019). Assessment of surface water resources in eastern Iraq. *Hydrology, 6*(3), 57.

Schaaf, C., & Wang, Z. (2021). MODIS/Terra+ Aqua BRDF/Albedo Daily L3 Global—500m V061 [Data set]. *NASA EOSDIS Land Processes DAAC*.https://doi.org/10.5067/MODIS/MCD43C3.061

Smith, S. M., and Edwards, E. C. (2021). Water storage and agricultural resilience against drought: historical evidence of the capacity and institutional limits of the United States. *Environmental Research Letters, 16*(12), 1240–1240, 2012.

Svoboda, M., Hayes, M., & Wood, D. (2012). Standardised precipitation index: user guide.

UNESCWA. (2013). *Inventory of shared water resources in Western Asia. Beirut: United Nations*. Retrieved January 13, 2025, from https://www.unescwa.org/publications/inventory-shared-water-resources-western-asia

Van Loon, A., and Laaha, G. (2015). Hydrological drought severity is explained by climate and catchment characteristics. *Journal of Hydrology, 526*, 3-14.

Xu, Z., Wu, Z., Shao, Q., He, H., & Guo, X. (2023). From meteorological to agricultural drought: Propagation time and probabilistic linkages. *Journal of Hydrology: Regional Studies, 46*, 101329.

Yang, X., Liao, X., Di, D., & Shi, W. (2023). A Review of Drought Disturbance on Socioeconomic Development. *Water, 15*(22), 3912.

Zeng, J., Li, J., Lu, X., Wei, Z., Shangguan, W., ZhangS. . . Zhang, S. (2022). Assessment of global meteorological, hydrological, and agricultural droughts under future warming based on CMIP6. *Atmospheric and Oceanic Science Letters, 15*(1), 100143.

Zhang, X., Schaaf, C. B., Friedl, M. A., Strahler, A. H., Gao, F., & Hodges, J. C. (2002). MODIS tasselled cap transformation and its utility. In *IEEE International Geoscience and Remote Sensing Symposium* (Vol. 2, pp. 1063-1065). IEEE.